

The temperature dependence of the yield stress for neutron-irradiated molybdenum

Meimei Li *, T.S. Byun, N. Hashimoto, L.L. Snead, S.J. Zinkle

Materials Science and Technology Division, Oak Ridge National Laboratory, Oak Ridge, TN 37831, United States

Abstract

Molybdenum was neutron-irradiated near 80 °C at doses of 7.2×10^{-5} , 7.2×10^{-4} , 7.2×10^{-3} , 0.072 and 0.28 dpa. Irradiated Mo was tensile tested over a temperature range of -50 to 100 °C at a strain rate of $1 \times 10^{-3} \text{ s}^{-1}$. It was found that the yield stress of irradiated Mo decreased at lower temperatures and increased at higher temperatures, resulting in reduced temperature dependence of yielding at lower doses (<0.001 dpa); the yield stress was increased, and the temperature dependence of yielding was nearly unchanged upon further irradiation at higher doses (>0.001 dpa). The temperature dependence of the yield stress for unirradiated and irradiated Mo is consistent with the theoretical expression of the Fleischer model for interactions of dislocations with tetragonal strain fields.

© 2007 Published by Elsevier B.V.

1. Introduction

Refractory metals have special importance for a number of innovative high technology applications. Molybdenum, in particular, is of great interest for high temperature applications in advanced fission and fusion reactor systems. It is attractive because of its high melting point, excellent high temperature strength, good thermal conductivity, and resistance to irradiation-induced swelling. Molybdenum also exhibits good corrosion resistance in liquid metals and in molten salts [1]. Therefore, it has potential applications in Gen IV systems, particularly in the liquid metal cooled fast reactor concepts and in molten salt coolant concepts. However, Mo, like

other body-centered cubic (bcc) metals is susceptible to irradiation embrittlement at low temperatures, leading to an increase in ductile–brittle transition temperature (DBTT). This embrittlement has imposed limitations on its low temperature applications, and has restricted its applications in nuclear energy systems.

The temperature dependence of the yield stress at low temperatures is the chief factor that influences the DBTT in bcc metals. Low temperature deformation of bcc metals is characterized by a strong temperature dependence of the yield stress as well as the strain rate dependence. This is in marked contrast to face-centered cubic (fcc) metals which exhibit a much weaker dependence of yielding on test temperature. The temperature dependence of the yield stress has been studied for both irradiated fcc and bcc metals. The temperature dependence of the flow stress for fcc metals, which is weak in the

* Corresponding author. Fax: +1 865 241 3650.
E-mail address: liml@ornl.gov (M. Li).

unirradiated condition, increases significantly upon neutron irradiation [2,3]. The temperature dependence of the flow stress in bcc metals, which is already strong in the unirradiated condition, is complex and still unclear in the irradiated condition. High solubility of interstitial impurities in bcc metals has also presented a great challenge in studies of thermally activated flow stress analysis, in both unirradiated and irradiated conditions. Investigations of the effect of neutron damage on the temperature dependence of yielding in bcc metals and alloys have indicated that the rate-controlling mechanisms of plastic deformation may or may not change as a result of neutron irradiation. For example, the temperature dependence of the yield stress in neutron-irradiated vanadium, niobium, and iron can increase, decrease or not change, depending on the purity, grain size, neutron dose, irradiation temperature, etc. [4–11].

This paper presents the temperature dependence of the yield stress over the temperature range of -50 to 100 °C of polycrystalline Mo irradiated at 80 °C to various doses. The effects of test temperature on radiation hardening were analyzed using a theoretical model.

2. Experimental procedure

The material examined was low carbon arc cast (LCAC) molybdenum, $>99.95\%$ purity with interstitial impurity contents of 140 ppm C, 6 ppm O and 8 ppm N. Subsize SS-3 sheet tensile specimens and rectangular coupon specimens were electro-discharge-machined from a cold-rolled 0.5 mm thick sheet. The tensile specimens had gauge dimensions of $7.62 \times 1.52 \times 0.50$ mm with an overall length 25.4 mm. The coupon specimens had dimensions of $25.4 \times 4.95 \times 0.25$ mm, and were used for microstructural characterization after irradiation. Following machining, specimens were annealed at 1200 °C for 1 h, resulting in an equiaxed grain structure with a grain size of 70 μm .

Irradiation of specimens was carried out in the hydraulic tube facility of the High Flux Isotope Reactor at the Oak Ridge National Laboratory. Specimens were loaded in perforated rabbit capsules allowing contact with the flowing coolant in the hydraulic tube to maintain the specimen temperature at ~ 80 °C. Specimens were irradiated to neutron fluences in the range of 2×10^{21} – 8×10^{24} n/m² ($E > 0.1$ MeV), corresponding to displacement dam-

age levels of 7.2×10^{-5} , 7.2×10^{-4} , 7.2×10^{-3} , 7.2×10^{-2} and 0.28 dpa.

Electrical resistivity of the tensile specimens was measured at room temperature before and after irradiation using a four-point probe technique. As-irradiated microstructure was examined using transmission electron microscopy (TEM). A detailed description of microstructural characterization can be found in a previous paper [12]. Tensile tests were conducted on unirradiated and irradiated specimens at a strain rate of 1.1×10^{-3} s⁻¹ at temperatures of -50 , -25 , 22 and 100 °C in air or a mixed air and cold nitrogen environment. The unirradiated material was also tensile-tested at -100 and 300 °C. Load and displacement data were recorded and used to determine stress–strain curves and tensile properties.

3. Results

3.1. As-irradiated microstructure

The defect structure of neutron-irradiated Mo was characterized by TEM and described in detail previously [12]. The following provides a brief summary of the results that are relevant to this study.

The major types of defect structure in neutron-irradiated Mo are loops, rafts and perhaps cavities. A low number density of defect clusters visible by TEM was observed in the 0.00072 dpa specimen. As the dose increased, both density and size of defect clusters increased significantly. The defect clusters were distributed homogeneously in the matrix up to 0.0072 dpa, and strong segregation of defect clusters and formation of rafts occurred at 0.072 dpa. The loop density increased only slightly from 0.0072 to 0.072 dpa and then decreased with increasing dose to 0.28 dpa. Possible cavity formation occurred at 0.28 dpa. The formation of defect clusters in neutron-irradiated Mo exhibited a non-linear dose accumulation rate and size dependence, which implies that diffusive nucleation and growth is the dominant process in defect cluster formation. Impurity trapping in the polycrystalline Mo was found to be more effective compared with high purity single crystal Mo [13], resulting in denser and finer clusters in the polycrystalline Mo.

3.2. Temperature dependence of the yield stress of unirradiated Mo

The engineering stress–strain curves for unirradiated Mo over the temperature range of -100 to

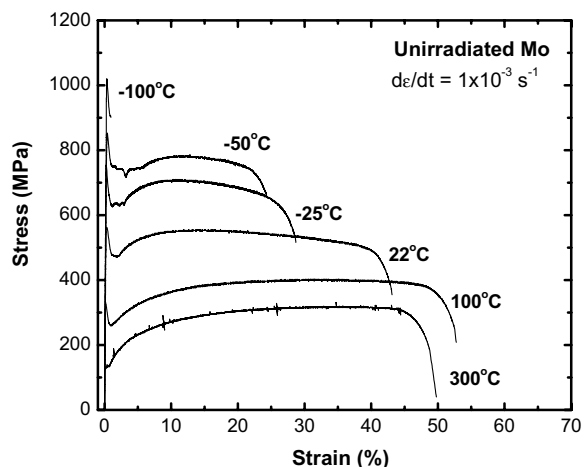


Fig. 1. Engineering stress–strain curves of unirradiated LCAC Mo tested between -100 and 300 °C at a strain rate of $1 \times 10^{-3} \text{ s}^{-1}$.

300 °C are shown in Fig. 1. The stress–strain curves illustrate the development of a yield point characterized by an enlarged yield elongation zone with decreasing temperature, followed by localized flow at yield at -100 °C. The lower yield stress (and the maximum stress at -100 °C) of unirradiated Mo is plotted as a function of test temperature in Fig. 2 along with the yield stress data of annealed Mo from the literature [14,15]. The yield stress of annealed Mo increased rapidly with decreasing temperature. The yield stress apparently reached the athermal regime at 150 – 200 °C (0.15 – $0.16T_m$, where T_m is the melting point for Mo). The yield stress of LCAC Mo examined in this study was relatively higher than the yield stress of annealed Mo studied

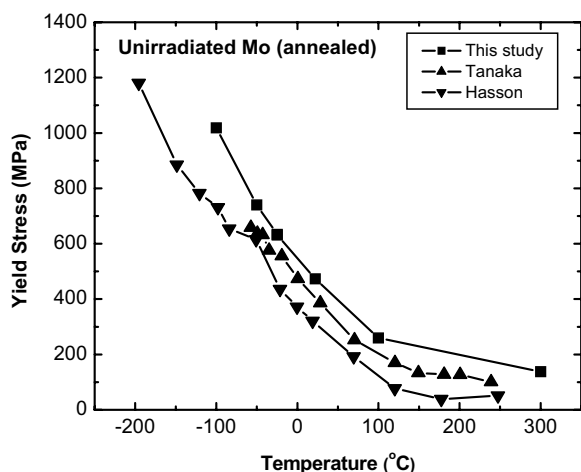


Fig. 2. Temperature dependence of the yield stress for unirradiated Mo.

by Tanaka et al. [14] and single crystal Mo by Hasson et al. [15]. This difference is likely associated with the material's processing, purity and strain rate. It should be mentioned that the data reported by Hasson et al. was for single crystal Mo of $[110]$ orientation. The values of the critical resolved shear stress were multiplied by 3.06 so to compare with the yield stress of polycrystalline materials. The polycrystalline Mo used in Tanaka and co-workers' investigation had similar purity and grain structure to the Mo examined in the present work.

3.3. Temperature dependence of the yield stress of neutron-irradiated Mo at lower doses

The engineering stress–strain curves for LCAC Mo neutron-irradiated to doses of 7.2×10^{-5} – 0.28 dpa over the temperature range of -50 to 100 °C are shown in Fig. 3. Note that the stress–strain curves of 7.2×10^{-5} and 7.2×10^{-4} dpa specimens are characterized by well-defined yield points and evident strain hardening. No early onset of plastic instability at yield was observed in these examined conditions. The stress–strain curves of irradiated Mo at 0.0072 dpa show a yield point and minimal strain hardening between -25 and 100 °C, while the specimen failed in a brittle manner at -50 °C. As dose increased, the brittle behavior is manifested, and the specimens failed in a brittle mode even at -25 °C at 0.072 dpa. Due to the anticipated embrittlement of the higher dose specimens, the specimens irradiated to 0.072 and 0.28 dpa were tested only at 22 and 100 °C. Plastic instability at yield was observed in these conditions. As various stress–strain curve behavior was observed in the irradiated specimens, a consistent determination of the yield stress is difficult. Three criteria were used to define the yield stress: (1) the lower yield stress for the curves showing a yield point; (2) the lower yield stress was estimated as the stress defined by the intersection of the lines drawn through the yield drop and the subsequent necking for curves showing plastic instability at yielding [16]; and (3) the maximum stress for the curves showing brittleness with total elongation $<0.5\%$.

Fig. 4 shows the temperature dependence of the lower yield stress for Mo irradiated to 7.2×10^{-5} and 7.2×10^{-4} dpa. The yield stress data for unirradiated and neutron-irradiated Mo to 4.8×10^{-4} and 7.7×10^{-4} dpa near room temperature from Tanaka et al.'s investigation are included in Fig. 4 for comparison [14]. It was found that the yield stress and its temperature dependence were slightly affected

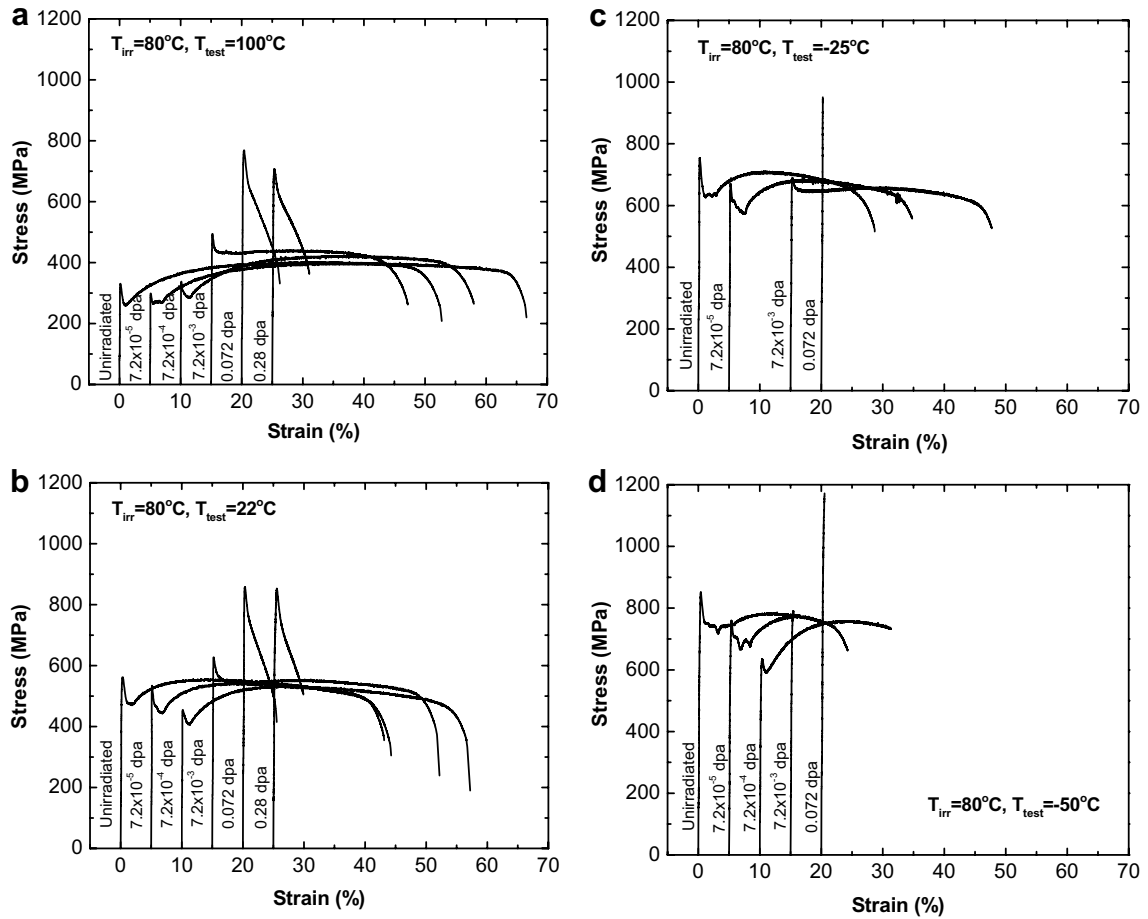


Fig. 3. Engineering stress–strain curves for neutron-irradiated LCAC Mo tested at (a) 100 °C, (b) 22 °C, (c) –25 °C and (d) –50 °C.

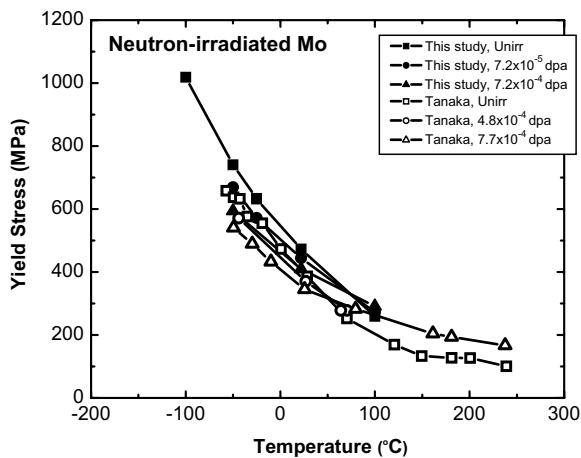


Fig. 4. Temperature dependence of the yield stress for neutron-irradiated Mo at doses of 7.2×10^{-5} and 7.2×10^{-4} dpa.

by neutron irradiation. Reduced temperature dependence was observed both in this study and in

the work of Tanaka et al. due to radiation-induced softening (decrease in yield stress) at low temperatures and hardening (increase in yield stress) at higher temperatures. The crossover of radiation softening and radiation hardening is ~ 70 °C in the present work and ~ 50 °C in Tanaka's experiments. The softening effect at lower temperature and hardening observed at 100 °C was stronger at 7.2×10^{-4} dpa than at 7.2×10^{-5} dpa for LCAC Mo, resulting in less temperature dependence for the 7.2×10^{-4} dpa specimen. Similarly, the Mo specimens irradiated to 7.7×10^{-4} dpa showed a smaller temperature dependence of yielding than the 4.8×10^{-4} specimens in the Tanaka et al. study.

3.4. Temperature dependence of the yield stress of neutron-irradiated Mo at higher doses

The temperature dependence of the yield stress for Mo irradiated to doses of 0.0072, 0.072 and

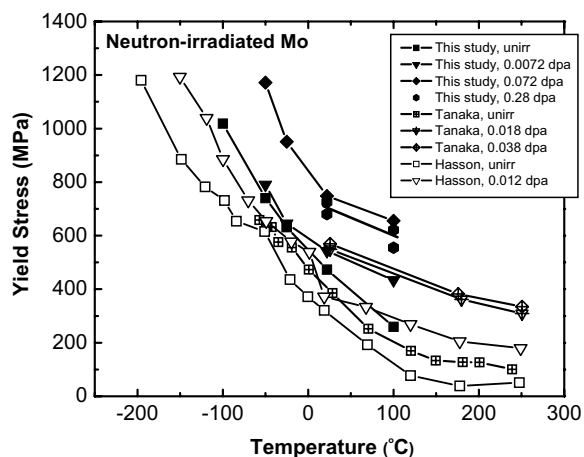


Fig. 5. Temperature dependence of the yield stress of neutron-irradiated Mo at doses between 7.2×10^{-3} and 0.28 dpa.

0.28 dpa is shown in Fig. 5. The effect of neutron irradiation on the temperature dependence of the yield stress is significantly different at higher doses. Only radiation hardening was observed and the dependence of the yield stress on test temperature was nearly unchanged in the dose range examined. The temperature dependence of yielding for irradiated LCAC Mo was compared with the results reported by Tanaka et al. [14] and by Hasson et al. [15]. The observations on the change in yield stress in irradiated Mo by Tanaka et al. are consistent with the findings in the present experiments. Hasson et al.'s data on neutron-irradiated single crystal Mo of [110] orientation showed that the increase in the yield stress after neutron irradiation is practically athermal in nature with a slight increase in temperature dependence at lower temperatures. It should be mentioned that the radiation effect on yielding of single crystal Mo is orientation-dependent. Hasson et al. found that both [110] and [491] oriented specimens showed radiation hardening at temperatures between 77 and 523 K, while the specimens of [100] orientation showed radiation softening over the temperature range of 190–250 and 300–400 K.

4. Discussion

The effect of neutron radiation on the temperature dependence of yielding in Mo falls into two groups depending on irradiation dose. In the low-dose irradiated Mo (<0.001 dpa) the temperature dependence of the yield stress was reduced upon

irradiation. The magnitude of reduction was larger at 7.2×10^{-4} dpa than at 7.2×10^{-5} dpa; in the high-dose irradiated Mo (>0.001 dpa), the temperature dependence of yielding was apparently not affected by irradiation, and temperature-insensitive hardening occurred. In order to understand the effect of neutron damage on the temperature dependence of yielding in irradiated Mo, it is necessary to consider the thermally activated deformation mechanisms in the unirradiated condition. The temperature dependence of the yield stress in bcc metals has been attributed to both intrinsic factors such as lattice resistance or the Peierls stress, and extrinsic factors such as interstitial impurities. A large amount of experimental evidence has shown that the temperature dependence of the yield stress decreases with increasing purity, but the temperature dependence is still substantial even in high purity bcc metals such as Fe, Nb, etc. [17–19]. The mechanism for overcoming the Peierls barrier by thermal fluctuation can be explained by the double-kink model [20,21], and the extrinsic hardening by interstitial impurities may be explained by the Fleischer model of interactions between dislocations and tetragonal strain fields [22,23].

In considering thermally activated flow processes in bcc metals, it is necessary to separate the flow stress into two components, an athermal stress component and a thermal stress component (also called the effective stress), i.e. $\sigma(T) = \sigma_{\text{ath}} + \sigma_{\text{th}}(T)$. Low temperature deformation in bcc metals is characterized by a rapidly decreasing stress with increasing temperature up to a critical temperature, T_0 , above which only athermal mechanisms control the plastic strain rate. The athermal stress, which is defined as the stress at the athermal temperature, T_0 , is weakly dependent on temperature through the shear modulus, but plays no role in the thermal activation process. The thermal stress component or the effective stress is related to short range barriers which a dislocation can overcome with the assistance of thermal energy, and it should be considered in the analysis of thermally activated deformation processes. The athermal stresses of irradiated and unirradiated Mo were estimated from the temperature dependence of the yield stress given in Figs. 4 and 5 for various irradiation doses by the apparent asymptotic stress approached as a function of increasing test temperature or by extrapolation to the asymptotic stress; the values of the athermal stress are given in Table 1. The thermal stress, which is the difference between the yield stress and the

Table 1

Estimated values of athermal stresses in irradiated and unirradiated Mo

Dose (dpa)	σ_{ath} (MPa)	Reference
Unirradiated	138	This study
0.0001	218	This study
0.001	243	This study
0.01	320	This study
0.1	524	This study
0.3	515	This study
Unirradiated	122	[14]
4.8e-4	196	[14]
7.7e-4	196	[14]
0.018	369	[14]
0.038	379	[14]
Unirradiated	38	[15]
0.012	178	[15]

athermal stress, is plotted as a function of test temperature in Fig. 6(a) for unirradiated and low-dose irradiated Mo (<0.001 dpa), and in Fig. 6(b) for unirradiated and high-dose irradiated Mo (>0.001 dpa). It is clearly seen that the thermal stress decreased upon neutron irradiation in low-dose irradiated Mo, while the thermal stress of the Mo irradiated to 0.0072 dpa and above is practically unchanged by neutron irradiation. It is also noted that the temperature dependence of the yield stress in high purity single crystal Mo with [1 10] orientation deviated from the trend below 200 K in the unirradiated condition, and the temperature dependence in irradiated single crystal Mo is slightly increased after irradiation to 0.012 dpa below 173 K. The athermal stresses of the single crystal Mo are significantly lower than those for polycrystal Mo.

Fleischer [22,23] formulated an analytical expression for the temperature dependence of the flow stress based on the interaction of dislocations with tetragonal strain fields, which is given as:

$$\left(\frac{\tau^*}{\tau_0^*}\right)^{1/2} = 1 - \left(\frac{T}{T_0}\right)^{1/2}, \quad (1)$$

where τ^* is the effective shear stress, τ_0^* is the effective shear stress at 0 K, T_0 is the temperature at which $\tau^* = 0$. Barriers giving this type of interaction can be interstitials, di-vacancies, point defect-impurity complexes, or small dislocation loops. The data shown in Fig. 6 were fitted by Eq. (1), and the results are given in Fig. 7. The Fleischer model gives a good fit to the effective stress for the unirradiated and irradiated Mo examined in this study and by Tanaka et al. However, the experimental data for

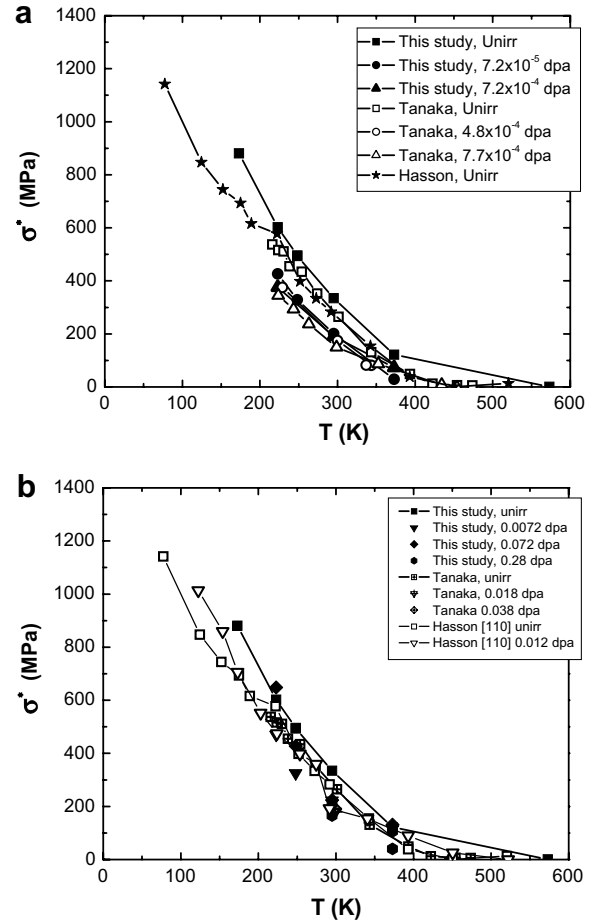


Fig. 6. Temperature dependence of the effective stress for unirradiated and neutron-irradiated Mo (a) at low-doses and (b) at high-doses.

unirradiated high purity single crystal Mo from Hasson et al. only showed good agreement with the Fleischer model between 140 and 320 K and progressively deviated from linearity below this temperature range. This implies that there may be an additional or an alternative mechanism operative, particularly in high purity Mo.

As the temperature-dependent yield stress of both unirradiated and irradiated Mo showed good agreement with the Fleischer model, the activation parameters may be determined by the Fleischer theory, i.e.

$$H = H_0 \left[1 - \left(\frac{\tau^*}{\tau_0^*}\right)^{1/2} \right]^2, \quad (2)$$

$$V^* = \frac{H_0}{\tau_0^*} \left[\left(\frac{\tau^*}{\tau_0^*}\right)^{1/2} - 1 \right], \quad (3)$$

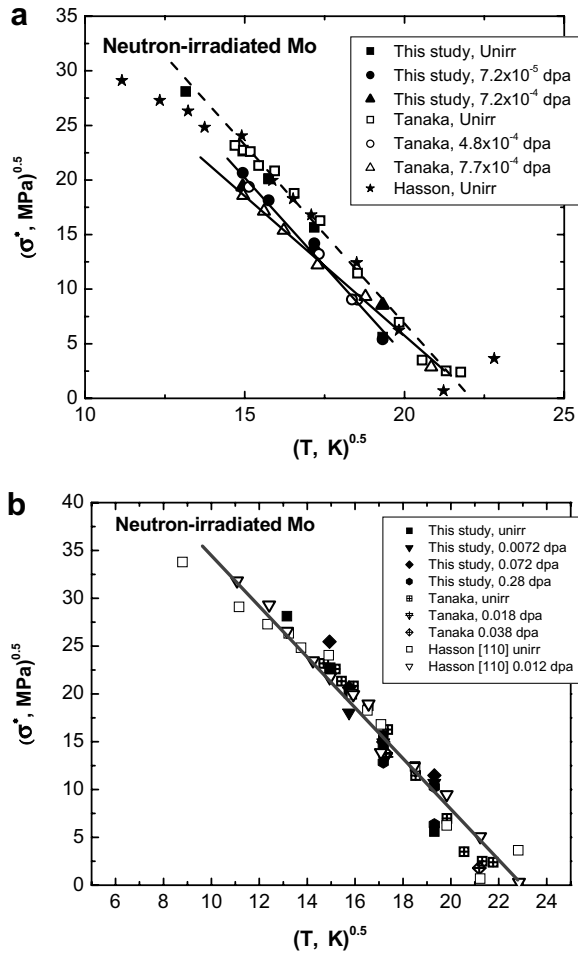


Fig. 7. Temperature dependence of the effective stress for unirradiated and neutron-irradiated Mo (a) at low doses and (b) at high-doses, showing the fit to the Fleischer model.

where H and V^* are the activation enthalpy and activation volume, respectively, and H_0 is the activation enthalpy at $\tau^* = 0$. The effective stress at 0 K, τ_0^* can be determined by the following expression:

$$\tau_0^* = \frac{\mu b}{2.6l}, \quad (4)$$

where μ is the shear modulus (140 GPa for Mo), b is the Burgers vector (0.273 nm), and l is the mean spacing between obstacles. The values of τ_0^* for Mo were estimated by extrapolating the temperature dependence curves of the yield stress to 0 K, and 1800, 1482 and 1178 MPa were obtained for unirradiated, 7.2×10^{-5} dpa, and 7.2×10^{-4} dpa irradiated Mo, respectively. A mean spacing of obstacle separation is estimated by Eq. (4) to be

25–38 nm. The microstructure characterization by TEM revealed a low number density of defect clusters at low-doses. From the data of the number density of visible defect clusters by TEM, the value of the mean spacing of defect clusters obtained for the 7.2×10^{-4} dpa specimen was 49 nm, close to the estimated values by Eq. (4). The activation enthalpy, H_0 , can be estimated by the maximum force exerted by the obstacle on a screw dislocation at 0 K, F_0 , and the obstacle diameter, d :

$$F_0 = \frac{\mu \Delta \epsilon b^2}{3.86}, \quad (5)$$

$$H_0 = \frac{F_0 d}{2}, \quad (6)$$

where $\Delta \epsilon$ is the tetragonal strain introduced into the lattice by the defect ($\Delta \epsilon = 1$ for a loop). From Eqs. (5) and (6), a value for H_0 of 8 eV is obtained for 1 nm size obstacles. The reduction in temperature dependence of yielding and decrease in the effective stress in low-dose irradiated Mo may be explained by the extrinsic ‘scavenging’ effect. Our early work [12] suggested that diffusive nucleation and growth is the controlling process in the formation of defect clusters in neutron-irradiated Mo. Neutron-produced defects may act as a trap for the impurity interstitials and remove the interstitial atoms from the solution, thereby decreasing the temperature dependence of yielding.

The temperature-insensitive radiation hardening in Mo irradiated to higher doses (>0.001 dpa) implies that irradiation to high-doses does not change the thermally activated deformation mechanism operative in the irradiated Mo. The barriers to dislocation motion produced during irradiation are largely athermal in character, i.e. they can not be surmounted easily as a result of thermal activation. Temperature-independent radiation hardening has been observed in other bcc metals. Smolik and Chen [8] reported that the increase in the yield stress of V by neutron irradiation to a fluence of 1.6×10^{18} n/cm² ($E > 1$ MeV) is independent of the test temperature between -153 and 25 °C. Wechsler et al. [6] found that the increase in the critical shear stress upon irradiation was approximately the same as of the unirradiated condition for single crystals of niobium over a range of temperatures from 93 to 298 K. Wechsler [5] suggested that the increase in the yield stress by neutron irradiation may depend on the material purity, and temperature-independent radiation hardening may occur only in low purity bcc metals, while increased temperature

dependence occurs in high purity irradiated bcc metals.

The athermal hardening effect in neutron-irradiated Mo may be evaluated by applying TEM measurements of defect density and mean size to the dispersed barrier model. The values of defect barrier strength, α for loops are 0.3–0.4 for doses of 0.1 dpa and above, and the critical force to surmount the barriers is about 0.3–0.4 μb^2 . It should be noted that plastic instability at yield was observed in several specimens irradiated to high-doses, as illustrated by the engineering stress–strain curves in Fig. 3. The localized flow upon yielding was explained by dislocation channeling in bcc metals including Mo [15,24]. Detailed discussion regarding the effect of dislocation channeling on thermal and athermal stresses of bcc metals is lacking in the literature.

5. Conclusions

The yield stress of Mo increased significantly after neutron irradiation at doses >0.001 dpa and an irradiation temperature of 80 °C. The temperature dependence of the yield stress is apparently unchanged upon irradiation, and the effect of neutron damage is essentially athermal in nature. When irradiated at lower doses (<0.001 dpa), the temperature dependence of yielding of Mo was reduced. Radiation softening occurred at lower temperatures, and radiation hardening occurred at higher temperature with a crossover temperature of 50–70 °C. The temperature dependence of the yield stress for unirradiated and irradiated Mo agrees with the Fleischer model of interactions of dislocations with tetragonal strain fields for low purity polycrystal Mo but not for high purity single crystal Mo.

Acknowledgements

The research was sponsored by the Office of Fusion Energy Sciences, the US Department of Energy under contract DE-AC05-00OR22725 with Oak

Ridge National Laboratory, managed and operated by UT-Battelle, LLC. We thank J.L. Bailey, A.M. Williams, L.T. Gibson and P.S. Tedder for their technical support.

References

- [1] J.H. DeVan, J.R. Distefano, E.E. Hoffman, in: Proceedings of Symposium on Refractory Alloy Technology for Space Nuclear Power Applications, Oak Ridge National Laboratory, 1983, p. 34 (August 10–11).
- [2] J. Diehl, in: A. Seeger et al. (Eds.), Vacancies and Interstitials in Metals, North-Holland, Amsterdam, 1969, p. 739.
- [3] T.J. Koppelaar, R.J. Arsenault, Metall. Rev. 157 (1971) 175.
- [4] E.A. Little, Int. Met. Rev. 21 (1976) 25.
- [5] M.S. Wechsler, Defect. Refract. Met. (1971) 257.
- [6] M.S. Wechsler, R.P. Tucker, R. Bode, Acta Metall. 17 (1969) 541.
- [7] P.R.V. Evans, A.F. Weinberg, R.J. Van Thyne, Acta Metall. 11 (1963) 143.
- [8] G.R. Smolik, C.W. Chen, J. Nucl. Mater. 35 (1970) 94.
- [9] H. Matsui, H. Shimidzu, S. Ta, M.W. Guinan, J. Nucl. Mater. 155–157 (1988) 1169.
- [10] K. Kitajima, H. Abe, Y. Aono, E. Kuramoto, J. Nucl. Mater. 108&109 (1982) 436.
- [11] R.J. Arsenault, E. Pink, Mater. Sci. Eng. 8 (1971) 141.
- [12] Meimei Li, N. Hashimoto, T.S. Byun, L.L. Snead, S.J. Zinkle, J. Nucl. Mater. (2005) (ICFRM-12).
- [13] B.N. Singh, J.H. Evans, A. Horsewell, P. Toft, G.V. Muller, J. Nucl. Mater. 258–263 (1998) 865.
- [14] M. Tanaka, K. Fukaya, K. Shiraishi, Trans. JIM 20 (1979) 697.
- [15] D.F. Hasson, Y. Huang, E. Pink, R.J. Arsenault, Metall. Trans. 5 (1974) 371.
- [16] L.L. Snead, S.J. Zinkle, D.J. Alexander, A.F. Rowcliffe, J.P. Robertson, W.S. Eatherly, Fusion Materials Semiann. Prog. Report, DOE/ER-0313/23, Oak Ridge National Lab, 1997, p. 81.
- [17] D.F. Stein, J.R. Low, Acta Metall. 14 (1966) 1183.
- [18] D.F. Stein, J.R. Low Jr., A.U. Seybolt, Acta Metall. 11 (1963) 1253.
- [19] K.V. Ravi, R. Gibala, Scripta Metall. 3 (1969) 521.
- [20] J.E. Dorn, S. Rajnak, Trans. AIME 230 (1964) 1052.
- [21] R.J. Arsenault, Acta Metall. 15 (1966) 501.
- [22] R.L. Fleischer, J. Appl. Phys. 33 (1962) 3504.
- [23] R.L. Fleischer, Acta Metall. 10 (1962) 835.
- [24] A. Luft, Prog. Mater. Sci. 35 (1991) 98.